波 谱 学 杂 志

第 36 卷第 2 期 Vol. 36 No. 2
2019 年 06 月 Chinese Journal of Magnetic Resonance Jun. 2019

Chinese J Magn Reson, 2019, 36(2): 127-137 doi:10.11938/cjmr20182659

天眷波谱青年论坛优秀主讲人特邀稿件

A Magnetic Resonance-Fluorescent Dual-Mode Imaging Probe for Stem Cell Tracking

ZHAO Min-min[1,2], *ZHANG Yan-hui*[2], *ZHANG Peng-li*[2], *TAN Bo*[2], *JIANG Hai-zhen*[1], *ZHANG Hai-lu*[2*], *DENG Zong-wu*[2#]

1. College of Sciences, Shanghai University, Shanghai 200444, China; 2. Suzhou Institute of Nano-Tech and Nano-Bionics, Chinese Academy of Sciences, Suzhou 215123, China

Abstract: A magnetic resonance (MR)-fluorescent dual-mode imaging probe was prepared by conjugating guaiazulene to Gd-DOTA, and used to label human mesenchymal stem cells (hMSCs) via electroporation. The probe self-assembled into nanoclusters in the cytoplasm, resulting in a significant reduction in T_2-weighted signal intensity that persisted up to 7 days. The fluorescence signal of the probe was observed at 498 nm, and the labelled hMSCs emitted a green fluorescence. The MR-fluorescent dual-mode imaging probe can potentially be used for stem cell tracking *in vivo*.

Key words: magnetic resonance imaging, fluorescent imaging, dual-mode probe, human mesenchymal stem cell

CLC number：O482.53 **Document code**：A

一种示踪干细胞的磁共振-荧光双模成像探针

赵敏敏[1,2]，张艳辉[2]，张朋利[2]，谭 波[2]，蒋海珍[1]，张海禄[2*]，邓宗武[2#]

1. 上海大学 理学院，上海 200444；2. 中国科学院 苏州纳米技术与纳米仿生研究所，江苏 苏州 215123

摘要：本文设计并合成了 Gd 基磁共振-荧光双模成像探针——Gd-DOTA-PEG-GA，通过电穿孔的方式标记人源间充质干细胞（hMSCs）．电穿孔标记诱导细胞将探针组装成团簇状纳米粒子进入细胞质，显著延长其与细胞结合的时间，并呈现出明显的 T_2 信号减弱效应，且信号减弱效应可以持续 7 天以上．在水溶液中，该探针的发射带集中在 498 nm，并且荧光强度在一周内无明显衰减．该探针标记的细胞在荧光倒置显微镜下呈现绿色荧光．这些结果表明该探针可以作为磁共振-荧光双模成像探针用于干细胞示踪．

关键词：磁共振成像；荧光成像；双模探针；人源间充质干细胞

个人简介：张海禄博士，中国科学院苏州纳米技术与纳米仿生研究所研究员，2008 年博士毕业于中国科学院武汉物理与数学研究所．目前任江苏省核磁共振专业委员会副主任委员，中华放射学会磁共振物理与工程学组委员，中国晶体学会药物学专业委员会常务委员．他的研究领域主要为药物固态化学和纳米-生物界面物理．

Received date: 2018-06-06; **Available online:** 2018-07-31

Foundation item: the National Natural Science Foundation of China (31371010, 21673281); Funds from Youth Innovation Promotion Association of the Chinese Academy of Sciences (2012242); Key Research Project from the Ministry of Science and Technology of China (2017YFA0104300).

Corresponding authors: * Tel: +86-51-262872713, E-mail: hlzhang2008@sinano.ac.cn;
Tel: +86-51-262872559, E-mail:zwdeng2007@sinano.ac.cn.

Introduction

Stem cell transplantation is a potential treatment option to regenerate tissue or organ functions that are impaired by acute injury or chronic degenerate diseases. In this respect, *in vivo* tracking of the cell transplants is critical to obtain information on their *in vivo* fates[1]. Many *in vivo* imaging approaches have been investigated for potential application in *in vivo* cell tracking, including magnetic resonance imaging (MRI)[2-4], positron emission tomography (PET)[5,6], and optical imaging[7,8], etc. MRI is regarded as one of the most powerful tools for cell tracking due to its deep tissue penetration depth, high spatial resolution, and non-invasive nature. Optical imaging is inexpensive, sensitive, and provides excellent temporal resolution, but it is limited to a tissue penetration depth of a few millimeters. These two imaging approaches are thus complementary in many aspects.

Exogenous stem cells are usually labeled with a specific imaging probe in order to be distinguished from its host tissue. A superparamagnetic agent such as iron oxide nanoparticles[9,10] or a paramagnetic agent such as Gd chelates[11,12] is usually used as an MRI contrast agent (CA). Iron oxide nanoparticles are usually used as T_2 CA. Gd chelates are usually used as T_1 CA. Quantum dots[7], fluorescent proteins[8], or fluorescent small molecules[13-15] are usually used as optical imaging probes.

Recently, we have reported that[16-19] labeling of human mesenchymal stem cells (hMSCs) with Gd agents via electroporation (EP) can induce cell-assembly of the Gd agents into nanoclusters in the cytoplasm. Along with the simultaneously introduced free Gd agents, a T_1/T_2 dual-mode MR imaging strategy was developed for *in vivo* tracking of stem cell transplants. The strategy reveals abundant information on *in vivo* fates of the cells. However, Gd agents have long been used as T_1 contrast agents. Their T_2 performance, particularly the T_1/T_2 dual-mode performance, needs to be cross examined by other imaging approaches.

For this purpose, we designed and synthesized a Gd-based MR-fluorescent dual-mode imaging probe. Although MR-fluorescent imaging probe have been reported which usually used traditional fluorescent dye as fluorescent group[13–15], we decided to couple Gd-DOTA with a simple small fluorescent molecule guaiazulene, 1,4-dimethyl-7-isopropyl azulene (GA). GA is a dark blue extract from gorgonian acanthogorgia species with high yield[20], and was selected as our fluorescent probe because its color can be easily changed via chemical functionalization[21,22]. Here we report our preliminary results on this work.

1 Materials and methods

1.1 Materials

1,4,7,10-tetraazacyclododecane hydrochloride was purchased from Shanghai Titan Scientific Co. Ltd. (China). GA was purchased from Jiangxi East Flavor & Fragrance Co. Ltd. (China). Other chemicals were purchased from Sinopharm Chemical Reagent Company (China). All chemicals are of analytical grade. Cell viability assay kit (MTT) was purchased from Beyotime (China). Fetal bovine serum (FBS), DMEM-F12 medium, penicillin-streptomycin, pancreatin, and all other cell culture related reagents were purchased from Gibco (USA). Milli-Q water (18.2 MΩ·cm) was used throughout the experiments and the system was purchased from Merck Millipore (China).

1.2 Synthesis of Gd-DOTA-PEG-GA

1-(acetic acid)-4,7,10-tris(tert-butoxycarbonyl methyl)-1,4,7,10-tetraazacyclodo-decane [DOTA(OtBu)$_3$] was synthesized from hydrochloride with a multistep procedure as described in literature[23].

2-(5-Isopropyl-3,8-dimethylazulen-1-yl)-2-oxoacetic acid (GA-C_2HO_3) was synthesized by chloroacetylation of GA as described by Wang et al.[24]

Fig. 1 illustrates the specific coupling process of DOTA and GA. The final DOTA-PEG-GA was purified by high performance liquid chromatography (HPLC) with purity >95%. Gadolinium chelating of DOTA-PEG-GA was conducted according to a previously reported procedure[16,17]. The molecular weight (*MW*) of the target product Gd-DOTA-PEG-GA was measured by electrospray ionization-mass spectrometry (ESI-MS, Agilent 1200/6220) for structural confirmation.

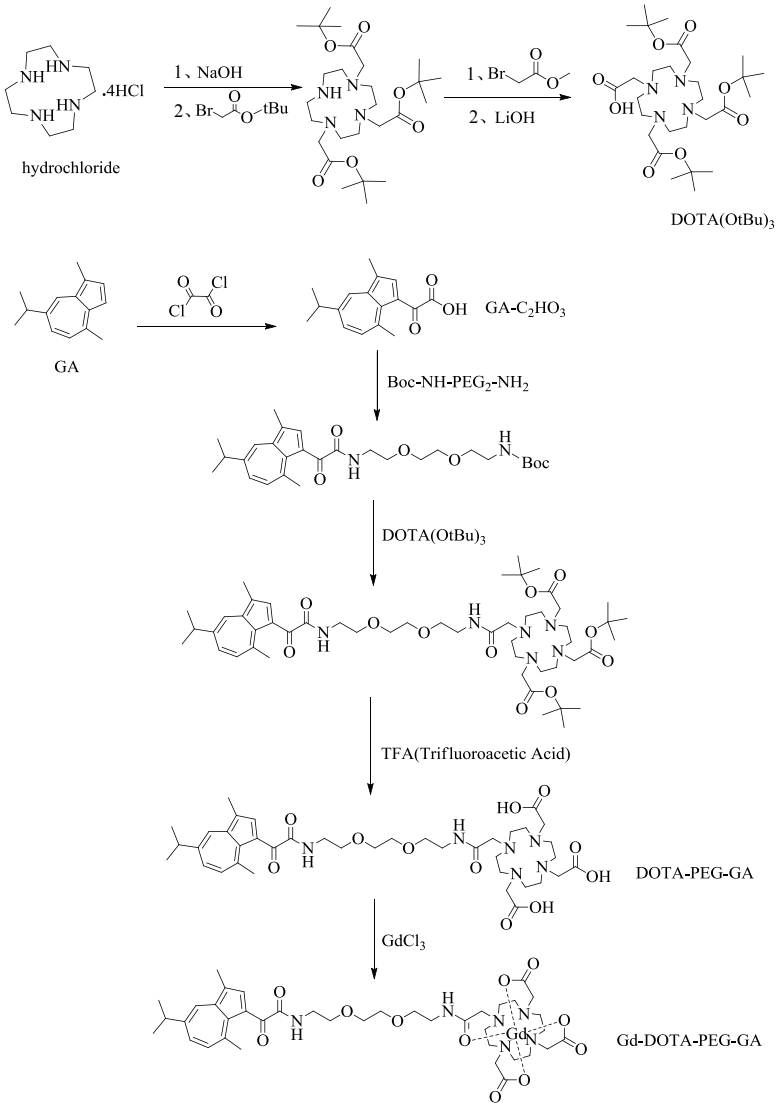

Fig. 1 Synthesis process of Gd-DOTA-PEG-GA

1.3 Fluorescence analysis of Gd-DOTA-PEG-GA

To investigate the fluorescent characteristic of Gd-DOTA-PEG-GA, fluorescence spectroscopy was performed with Gd-DOTA-PEG-GA dissolved in ultrapure water at concentration of 10 μmol/L in a 3 mL quartz cuvette of 1 cm path length. In addition, time-variations of fluorescence emission spectra of Gd-DOTA-PEG-GA during 0~7 days were also measured to determine its stability.

1.4 Relaxivity of aqueous Gd-DOTA-PEG-GA

MRI scans of aqueous Gd-DOTA-PEG-GA solutions were performed on a Bruker AVANCE 500WB spectrometer (Bruker Biospin, Germany) with an 89 mm vertical bore magnet of 11.7 T using a birdcage coil with *i.d.* of 15 mm at probe temperature of about 22 ℃. Gd-DOTA was used as a control throughout this work. Both T_1- and T_2-relaxation times with different Gd concentrations were measured. T_1- and T_2-relaxation rates were characterized by the reciprocal of T_1- and T_2-relaxation times, respectively. Gd concentration of the solutions was measured by inductively coupled plasma-mass spectrometry (ICP-MS, Thermo X Series2, USA). Aqueous r_1 and r_2 in unit of $mmol^{-1}$ ŁL s^{-1} were calculated through curve-fitting of T_1- and T_2-relaxation rates versus Gd concentrations (mol/L).

T_1-relaxation time was acquired by using RARE sequence with echo time (*TE*) = 7 ms; repetition time (*TR*) = 40, 70, 100, 180, 300, 500, 750, 1 000, 1 500, 3 000, 5 000 ms; field of view (*FOV*) = 12×12 mm^2; matrix = 96×96; slice thickness/gap = 0.8/0.2 mm; number of average = 2. T_2-relaxation time was acquired by using multi slice multi echo (MSME) sequence with *TR*=3 000 ms, *TE*=8~480 ms, *FOV*=12×12 mm^2, matrix=96×96, slice thickness/gap = 0.8/0.2 mm, and number of average = 2.

1.5 EP-labeling of hMSCs with Gd-DOTA-PEG-GA

hMSCs were seeded into 100 mm × 20 mm style cell culture dishes at a density of about 1×10^6 cells per dish and maintained for 24 h at 37 ℃. Cells were trypsinized and centrifuged at 1 000 rpm for 5 min. The precipitated cells were resuspended in 200 μL EP-buffer in the presence of Gd-DOTA-PEG-GA at probe concentrations between 0~10 mmol/L, and were transferred to 96-well plates, respectively. Six electrical pulses of 100 μs at about 120 V and an interval of 1 s were then applied to the cells using X-Porator® EBXP-H1 (Etta Biotech, China). After EP-labeling, the cells were collected and suspended in 4 mL DMEM-F12, and allowed to recover for 15 min.

1.6 MTT cytotoxicity assay

Cell viability of hMSCs after EP-labeling with Gd-DOTA-PEG-GA was assessed by MTT assay. hMSCs were suspended in 200 μL EP-buffer containing 0, 1, 2, 5 and 10 mmol/L of Gd-DOTA-PEG-GA, respectively. Defined electrical pulses were applied to the cells. hMSCs without any probe labeled were treated as control. After EP-labeling, the cells were collected and suspended in 4 mL DMEM-F12, rinsed twice with 4~6 mL PBS, and transferred into a 96-well plate (8×10^3 cells per well). *In vitro* cell viability of Gd-DOTA-PEG-GA labeled hMSCs was assessed by using a standard MTT cytotoxicity assay. Each experiment was repeated five times. Statistical significance was evaluated using *t*-test ANOVA analysis. $p<0.05$ was considered to indicate a statistically significant difference.

1.7 TEM of hMSCs labeled with Gd-DOTA-PEG-GA

Cellular transmission electron microscopy (TEM) was performed to precisely localize the Gd-DOTA-PEG-GA distribution in hMSCs. Labeled hMSCs were transferred into a microcentrifuge tube and spun at 1 000 rpm for 5 min. The supernatant was removed, and 1 mL 2.5% glutaraldehyde buffered with PBS was added into the microcentrifuge tube to fix hMSCs at 4 ℃ overnight. Afterwards, the cell mass was embedded in 5% agar gel and fixed in 2.5% glutaraldehyde buffered with PBS at 4 ℃ at least for 6 h followed by washing with PBS twice. Cells were then fixed in 1% osmium tetraoxide buffered with PBS for 1 h and washed three times with PBS. The samples were dehydrated using a series of acetone treatment (30%, 50%, 70%, 80%, 90%, 3×100%) of 15 min each, followed by embedded in 1∶1 epoxy resin/acetone solution for 1 h. The samples were then transferred into capsules containing fresh 100% epoxy resin and

fixed for at least 2 h. The capsules were then left in a furnace at a temperature of 70 ℃ for 2 days to polymerize the epoxy resin. After quickly cooling down, the hardened samples were cut into 70~90 nm thick sections with Ultramicrotome (Leica UC6, Austria) and applied on a copper grid for TEM observation (Tecnai G2 F20 S-Twin, FEI, USA).

1.8 *In vitro* MRI of hMSCs labeled with Gd-DOTA-PEG-GA

hMSCs labeled with Gd-DOTA or Gd-DOTA-PEG-GA at concentrations of 0, 2, 5, and 10 mmol/L were seeded in 100 mm × 20 mm dishes (about 1×10^6 cells/dish), respectively. When cell density growing to 90%, half of EP-labeled hMSCs were used for proliferation and the other half were treated for *in vitro* MRI. For MRI, hMSCs were trypsinized, centrifuged, and washed twice with PBS. The harvested cells were transferred into a capillary with *i.d.* of about 1.0 mm and packed into cell pellets by centrifugation at 1 200 rpm for 5 min. T_1- and T_2-weighted images of hMSC pellets were collected on the 11.7 T MRI system. T_1- and T_2-relaxation times were also measured.

T_1-weighted images were acquired by using MSME sequence with *TE* = 5.2 ms, *TR* = 500 ms, *FOV* = 12×12 mm^2, matrix = 96×96, slice thickness/gap = 0.8/0.2 mm, and number of average = 4. T_2-weighted images were acquired by using MSME sequence with *TE* = 40 ms, *TR* = 3 000 ms, *FOV* = 12×12 mm^2, matrix = 96×96, slice thickness/gap = 0.8/0.2 mm, and number of average = 2.

1.9 *In vitro* fluorescence imaging of EP-labeled hMSCs

For *in vitro* tracking of hMSCs by fluorescence imaging, hMSCs were EP-labeled with Gd-DOTA-PEG-GA at a concentration of 5 mmol/L. After EP-labeling, the cells were collected and suspended in 4 mL DMEM-F12, allowed to recover for 15 min, and then transferred into 100 mm×20 mm dishes for incubation and proliferation. After washing with PBS for 3 times, the cells were observed under an inverted microscope (Nikon Ti-E microscopy, Japan).

2 Results and discussion

2.1 MS characterization of Gd-DOTA-PEG-GA

The chemical structure of Gd-DOTA-PEG-GA was confirmed by their *MW* as measured by ESI-MS. Fig. 2 shows mass spectrum of Gd-DOTA-PEG-GA ($C_{39}H_{55}GdN_6O_{11}$, *MW* = 941.32), found at *m*/*z* 471.664 0 for $[M+2H]^{2+}$.

2.2 Relaxivity of aqueous Gd-DOTA-PEG-GA

Fig. 3 presents T_1- and T_2-relaxation rates of Gd-DOTA and Gd-DOTA-PEG-GA solutions as a function of Gd concentration. r_1 and r_2 of Gd-DOTA are about 3.74 and 4.85 mmol^{-1} Ł s^{-1}. r_1 and r_2 of Gd-DOTA-PEG-GA are about 5.65 and 7.74 mmol^{-1} Ł s^{-1}, respectively, both slightly higher than that of Gd-DOTA.

2.3 Fluorescence spectroscopy

Fig. 4(a) shows the fluorescence excitation and emission spectra of Gd-DOTA-PEG-GA at concentrations of 10 μmol/L. An absorption band was observed at 425 nm and an emission band was observed at 498 nm upon excitation at a wavelength of 425 nm. Both the emission band shape and intensity remain stable during a period of 7 days [Fig. 4(b)]. The results suggest that Gd-DOTA-PEG-GA was sufficiently stable for the use as MR-fluorescence dual-mode probe.

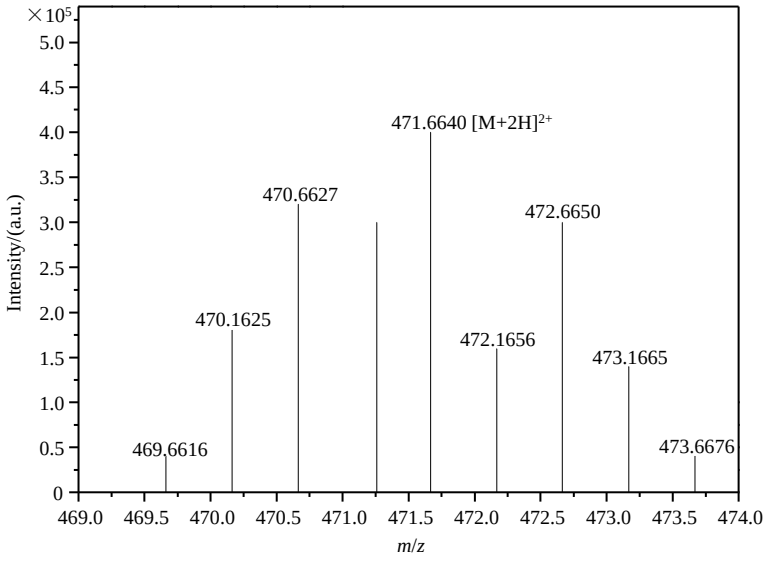

Fig. 2 Mass spectrum of Gd-DOTA-PEG-GA with fragmentation energy of 120.0 V in positive mode

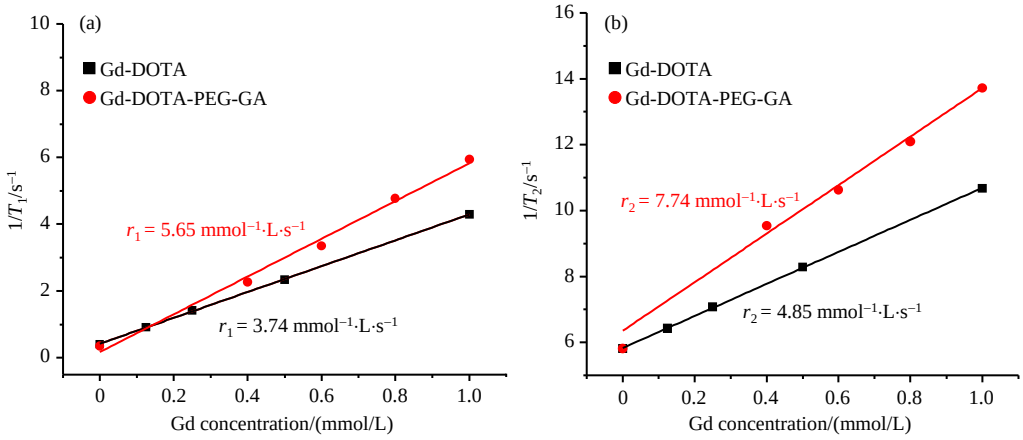

Fig. 3 (a) T_1- and (b) T_2-relaxation rates as a function of Gd concentration

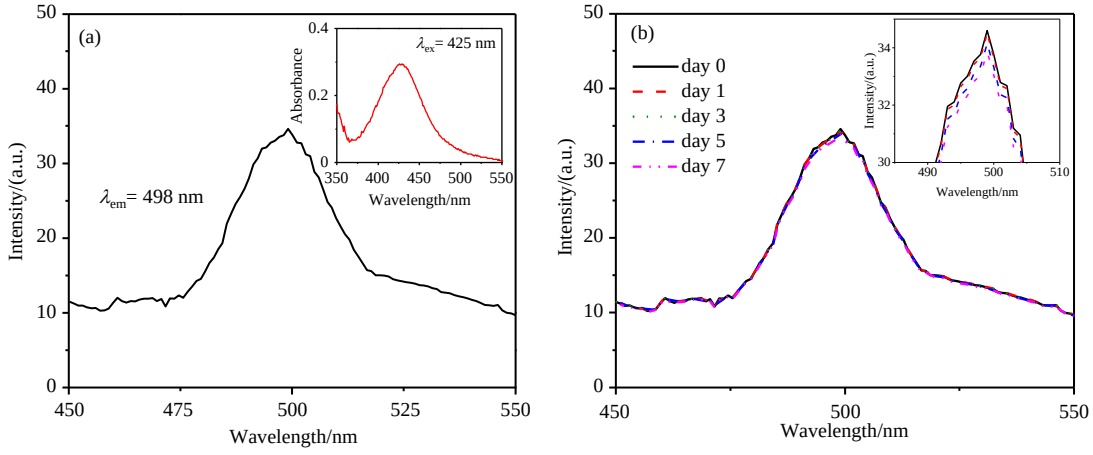

Fig. 4 (a) Fluorescence emission spectrum of 10 μmol/L Gd-DOTA-PEG-GA (inset, fluorescence excitation spectrum of Gd-DOTA-PEG-GA); (b) Fluorescence emission spectra of 10 μmol/L Gd-DOTA-PEG-GA in ultrapure water during 7 days

2.4 Cytotoxicity assessment

Fig. 5 illustrates possible cytotoxicity induced by either EP or the contrast agents. EP in the absence of Gd-DOTA-PEG-GA (EP0) exerted minor adverse effects on the survival of hMSCs with cell viability of about 95% relative to the control. EP1~EP10 in the presence of Gd-DOTA-PEG-GA at concentrations of 1, 2, 5, 10 mmol/L exerted minor additional adverse effects on hMSCs with cell viability of about 90% relative to the control. The results suggest that the contrast agent is biologically safe.

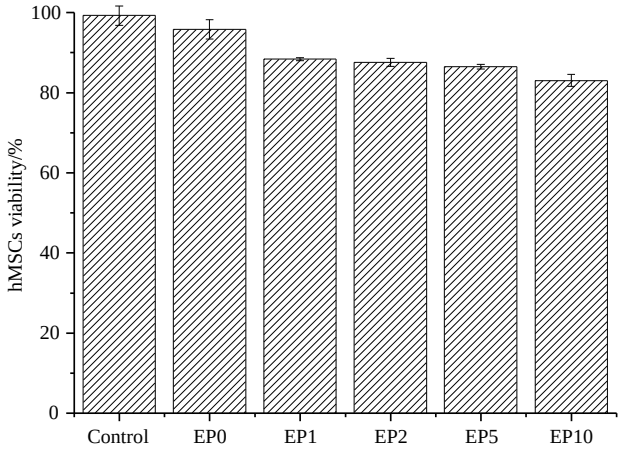

Fig. 5 MTT assay of hMSCs without any probe labeled (control) and EP-labeled with Gd-DOTA-PEG-GA at different concentrations (EP0: 0 mmol/L, EP1: 1 mmol/L, EP2: 2 mmol/L, EP5: 5 mmol/L, EP10: 10 mmol/L)

2.5 Cellular distribution of Gd-DOTA-PEG-GA in EP-labeled hMSCs

Fig. 6 presents TEM images of hMSCs EP-labeled with Gd-DOTA-PEG-GA which were subjected to fixed dehydration with 2.5% glutaraldehyde for 6 h at 4 ℃ on day 0, 1, 3 after cell labeling. EP-labeling of hMSCs induced cell-assembly of Gd-DOTA-PEG-GA nanoclusters into cytoplasm. Immediately after cell

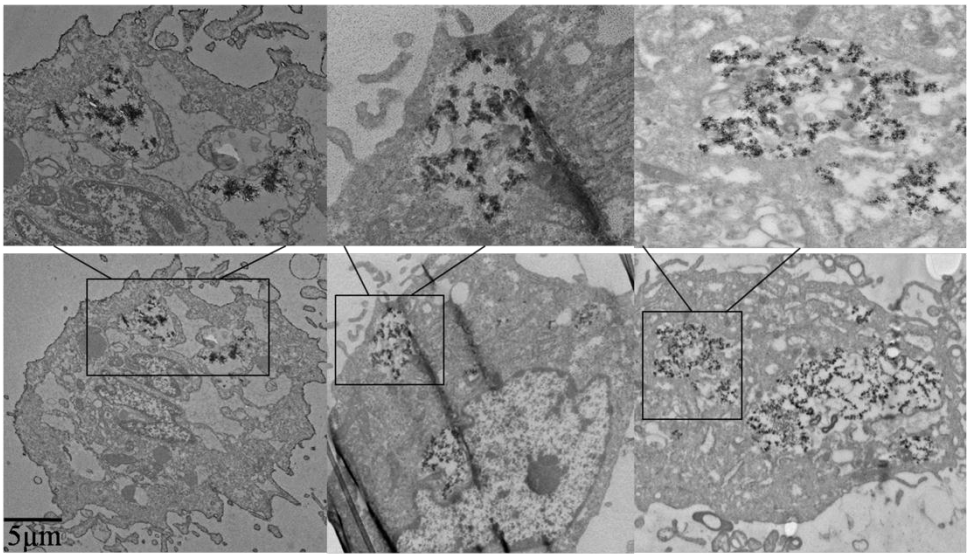

(a) (b) (c)

Fig. 6 Cellular TEM images of hMSCs EP-labeled with Gd-DOTA-PEG-GA: (a) Immediately after cell labeling; (b) Followed by a 1-day culture and recovery; (c) Followed by a 3-day culture and recovery. The scale bar is 5 μm

labeling (on day 0), both intracellular nanoclusters and membrane-bound Gd-DOTA-PEG-GA were observed [Fig. 6(a)]. In addition, we also noted that significant amount of free Gd-DOTA-PEG-GA agents were introduced to the cytoplasm during EP-labeling. On day 1 and day 3, membrane-bound Gd-DOTA-PEG-GA disappeared with only intracellular nanoclusters remaining in the cytoplasm [Fig. 6(b) and 6(c)]. The free Gd-DOTA-PEG-GA agents were also released quickly via exocytosis during cell culture. The findings suggest that the cell-assembled nanoclusters have longer cellular retention time than the membrane-bound Gd-DOTA-PEG-GA, in agreement with our previous findings on other MRI probes[17,19].

2.6 *In vitro* cellular MRI

Fig. 7 presents T_1- and T_2-weighted MR images of hMSCs EP-labeled with Gd-DOTA-PEG-GA at concentrations of 2, 5, and 10 mmol/L collected immediately after cell labeling as well as subsequently after cell proliferation of defined times. A bright signal appeared in both T_1- and T_2-weighted images of hMSCs EP-labeled with Gd-DOTA (as a control) but persisted only about 3 days. T_1-weighted images of hMSCs EP-labeled with Gd-DOTA-PEG-GA at different concentrations did not show obvious signal enhancement [Fig. 7(a)]. T_2-weighted images showed a dark signal that persisted for about 7 days [Fig. 7(b)].

The measured T_1- and T_2-weighted signal intensities of hMSCs are plotted as functions of cell proliferation time in Fig. 7(c) and 7(d). The measured T_1- and T_2-relaxation rates of hMSCs after MR image collection are also plotted as a function of cell proliferation time in Fig. 7(e) and 7(f), which can account for the measured changes in both T_1- and T_2-weighted signal intensities on the basis of Equ. (1)[17,25]:

$$F_{se} \propto (1-\mathrm{e}^{-T_\mathrm{R}/T_1})\mathrm{e}^{-T_\mathrm{E}/T_2} \tag{1}$$

where F_{se} is the spin echo signal intensity, $1/T_1$ and $1/T_2$ are T_1- and T_2-relaxation rates, T_R and T_E are experimental repetition time and echo time, respectively.

Labeling of hMSCs with an MRI contrast agent accelerates both T_1- and T_2-relaxation rates. Free Gd-DOTA agent introduced into the cytoplasm is in favor of acceleration of T_1-relaxation rate and thus MRI signal enhancement [Fig. 7(c) and 7(d), day 0 and day 1]. Subsequent fast release of free Gd-DOTA agent from the cytoplasm results in a fast recovery of T_1-relaxation rate [Fig. 7(e)] associated with a fast recovery of both T_1- and T_2-weighted signal [Fig. 7(c) and (d), day 4 and later]. EP induced cell-assembly of Gd-DOTA-PEG-GA nanoclusters into the cytoplasm is in favor of acceleration of T_2-relaxation rate and thus MRI signal reduction [Fig. 7(c) and 7(d), day 0 and day 1]. The intracellular nanoclusters have longer cellular retention time so that acceleration of T_2-relaxation rate can persist over a longer period which is associated with a persistent T_2-weighted signal reduction effect. The findings are also in agreement with our previous findings[17-19] on other MRI probes and thus suggest that the dual-mode probe can be used for *in vivo* MRI tracking of transplanted stem cells.

2.7 Fluorescence imaging

Fig. 8 presents fluorescence images of hMSCs EP-labeled with Gd-DOTA-PEG-GA at a concentration of 5 mmol/L under an inverted microscope. Bright field image confirmed that the cells were viable throughout the experiments after EP-labeling with Gd-DOTA-PEG-GA [Fig. 8(a)]. The nanoclusters were distributed within the cytoplasm, emitting green fluorescence under UV excitation [Fig. 8(b)]. Overlay of bright and dark field images demonstrates that the green fluorescence was from both the cell membrane and the intracellular region [Fig. 8(c)]. The results indicate the potential of Gd-DOTA-PEG-GA as a fluorescent nanoprobe.

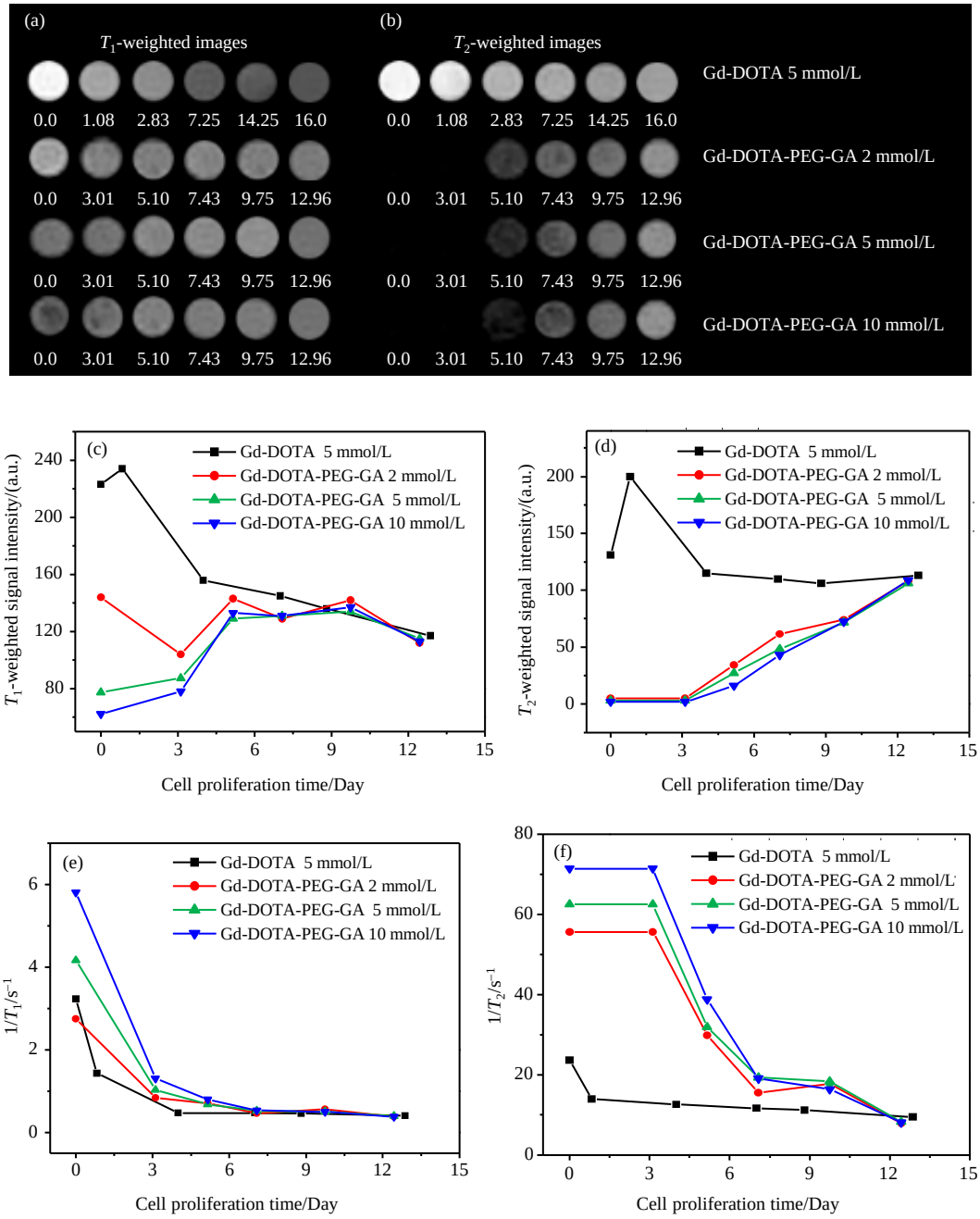

Fig. 7 *In vitro* (a) T_1- and (b) T_2-weighted MR images of hMSCs pellets EP-labeled with Gd-DOTA and Gd-DOTA-PEG-GA as a function of cell proliferation time at 11.7 T. Number below each image indicates cell proliferation time in day. (c) T_1- and (d) T_2-weighted MR signal intensities; (e) Cellular T_1- and (f) T_2-relaxation rates. MR signal intensity of dark image is tentatively given a value of 5 or below for ease of following its change profile (b). Discussion on T_2 relaxation rate has to be restricted to below 50 s^{-1} because the accuracy of measurement of T_2 relaxation rate deteriorates at above 50 s^{-1} (equivalent to T_2 relaxation time of below 20 ms)

Combining with its MRI performance, it can function as a MR-fluorescent dual-mode probe for stem cell tracking. For example, the T_2 effect of this probe can be used for the *in vivo* MRI observation, and optic property allows the straightforward hMSCs localization for a physiological section analysis without the necessity of cell staining.

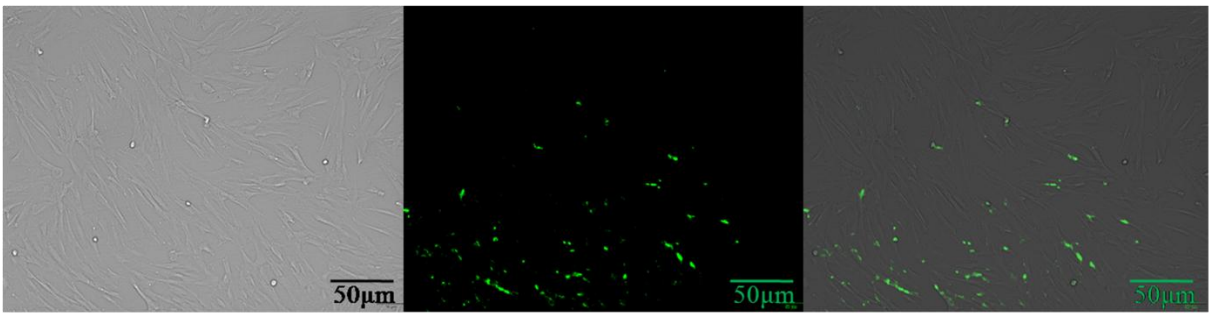

(a) (b) (c)

Fig. 8 Fluorescence images of hMSCs EP-labeled with Gd-DOTA-PEG-GA at a concentration of 5 mmol/L under inverted microscope: (a) Bright field; (b) Dark field; (c) Overlay of (a) and (b). The scale bar is 50 μm

3 Conclusion

Gd-DOTA was coupled with GA to yield an MR-fluorescent dual-mode imaging probe for stem cell tracking. The probe was used to label hMSCs via electroporation. EP-labeling induced cell-assembly of the probe into nanoclusters in the cytoplasm as confirmed by cellular TEM. Cellular MRI of EP-labeled hMSCs demonstrated a significant T_2-weighted signal reduction effect which persisted over 7 days. The probe has an UV absorption band at 425 nm, and a fluorescent band at 498 nm with good stability. hMSCs labeled with the probe exhibited a green fluorescence under inverted microscope. The biosafety was preliminarily assessed by MTT assay which yielded a high cellular viability for EP-labeling with the probe. These characteristics allow the probe to function as an MR-fluorescent dual-mode imaging probe for cell tracking.

Acknowledgement: The authors acknowledge Karebay Biochem Inc. for assistance with synthesis of DOTA-PEG-GA.

Reference:

[1] GERA A, STEINBERG G K, GUZMAN R. *In vivo* neural stem cell imaging: current modalities and future directions[J]. Regen Med, 2010, 5(1): 73-86.

[2] KRAITCHMAN D L, BULTE J W. Imaging of stem cells using MRI[J]. Basic Res Cardiol, 2008, 103(2): 105-113.

[3] POLITI L S. MR-based imaging of neural stem cells[J]. Neuroradiology, 2007, 49(6): 523-534.

[4] ROGERS W J, MEYER C H, KRAMER C M. Technology insight: *in vivo* cell tracking by use of MRI[J]. Nat Rev Cardiol, 2006, 3(10): 554-562.

[5] ZHANG H, SONG F H, XU C Y, et al. Spatiotemporal PET imaging of dynamic metabolic changes after therapeutic approaches of induced pluripotent stem cells, neuronal stem cells, and a Chinese patent medicine in stroke[J]. J Nucl Med, 2015, 56(11): 1774-1779.

[6] WANG J C, CHAO F F, HAN F, et al. PET demonstrates functional recovery after transplantation of induced pluripotent stem cells in a rat model of cerebral ischemic injury[J]. J Nucl Med, 2013, 54(5): 785-792.

[7] CHEN G C, TIAN F, LI C Y, et al. *In vivo* real-time visualization of mesenchymal stem cells tropism for cutaneous regeneration using NIR-II fluorescence imaging[J]. Biomaterials, 2015(53): 265-273.

[8] CHENG G C, LIN S Y, HUANG D H, et al. Revealing the fate of transplanted stem cells *in vivo* with a novel optical imaging strategy[J]. Small, 2018, 14(3). doi: 10.1002/smll.201702679.

[9] MAHMOUDI M, HOSSEINKHANI H, HOSSEINKHANI M, et al. Magnetic resonance imaging tracking of stem cells *in vivo* using iron oxide nanoparticles as a tool for the advancement of clinical regenerative medicine[J]. Chem Rev, 2011, 111(2): 253-280.

[10] ZHANG H Y, LI C L, YING X F, et al. A gadolinium-based T_1 MRI probe for detection of lung cancer stem cells [J]. Chinese J Magn Reson, 2016, 33(4): 627-634.
张宏岩, 李春林, 英晓芳, 等. 靶向肺癌干细胞的多肽 Gd 基 T_1 型 MRI 探针的研究[J]. 波谱学杂志, 2016, 33(4): 627-634.

[11] AGUDELO C A, TACHIBANA Y, HURTADO A F, et al. The use of magnetic resonance cell tracking to monitor endothelial progenitor cells in a

rat hindlimb ischemic model[J]. Biomaterials, 2012, 33(8): 2439-2448.

[12] TACHIBANA Y, ENMI J I, AGUDELO C A. et al. Long-term/ bioinert labeling of rat mesenchymal stem cells with PVA-Gd conjugates and MRI monitoring of the labeled cell survival after intramuscular transplantation [J]. Bioconjugate Chem, 2014, 25(7): 1243-1251.

[13] HUBER M M, STAUBLI A B, KUSTEDJO K, et al. Fluorescently detectable magnetic resonance imaging agents[J]. Bioconjugate Chem, 1998, 9(2): 242-249.

[14] KIM E J, BHUNIYA S, LEE H, et al. *In vivo* tracking of phagocytic immune cells using a dual imaging probe with gadolinium-enhanced MRI and near-infrared fluorescence[J]. ACS Appl Mater Interfaces, 2016, 8(16): 10266.

[15] ZHU T F, MA X Q, CHEN R H, et al. Using fluorescently-labeled magnetic nanocomposites as a dual contrast agent for optical and magnetic resonance imaging[J]. Biomater Sci, 2017, 5(6): 1090-1100.

[16] CAO L M, LI B B, YI P W, et al. The interplay of T_1- and T_2-relaxiation on T_1-weighted MRI of hMSCs induced by Gd-DOTA-peptides[J]. Biomaterials, 2014, 35(13): 4168-4174.

[17] ZHANG Y H, ZHANG H Y, LI B B, et al. Cell-assembled $(Gd\text{-}DOTA)_i$-triphenylphosphonium (TPP) nanoclusters as a T_2 contrast agent reveal *in vivo* fates of stem cell transplants[J]. Nano Res, 2018, 11(3): 1625-1641.

[18] ZHANG Y H, ZHANG H Y, ZHANG H L, et al. Preparation and application of a new-type Gd agents as T_2 contrast agent[J]. Chinese J Magn Reson, 2017, 34(3): 302-310.
张艳辉, 张宏岩, 张海禄, 等. 新型 Gd 基 T_2 造影剂的制备和应用[J]. 波谱学杂志, 2017, 34(3): 302-310.

[19] ZHANG P L, ZHANG Y H, LI B B, et al. Cell-assembled nanoclusters of MSC-targeting Gd-DOTA-peptide as a T_2 contrast agent for MRI cell tracking[J]. J Pept Sci, 2018, 24(4/5): e3077.

[20] CHEN D W, YU S J, OFWEGEN L V, et al. Anthogorgienes A-O, new guaiazilene-derived terpenoids from a Chinese gorgonian anthogorgia species, and their antifouling and antibiotic activities[J]. J Agric Food Chem, 2012, 60(1): 112-113.

[21] AMIR E, AMIR R J, CAMPOST L M, et al. Stimuli-responsive azulene-based conjugated oligomers with polyaniline-like properties [J]. J Am Chem Soc, 2011, 133(26): 10046-10049.

[22] DONG J X, ZHANG H L. Azulene-based organic function molecules for optoelectronics[J]. Chinese Chem Lett, 2016, 27(8): 1097-1104.

[23] LI C, WINNARD P, BHUJWALLA Z M. Facile synthesis of 1-(acetic acid)-4,7,10-tris(tert-butoxycarbonylmethyl)-1,4,7,10-tetraazacyclododecane: a reactive precursor chelating agent[J]. Tetrahedron Lett, 2009, 50(24): 2929-2931.

[24] WANG D L, HAN S, GU Z, et al. Synthesis of 1-(2-Benzo[b]furoyl) guaiazulene derivatives[J]. Chinese J Org Chem, 2008, 28(9): 1641-1645.
王道林, 韩珊, 谷峥, 等. 1-(2-苯并呋喃酰基)愈创兰烃奠的合成[J]. 有机化学, 2008, 28(9): 1641-1645.

[25] MCROBBIE D W, MOORE E A, GRAVES M J, et al. MRI from picture to proton[M]. 2nd ed. Cambrige: Cambrige University Press, 2007.